Ocular and Optical Coherence Tomography–Based Corneal Aberrometry in Keratoconic Eyes Treated by Intracorneal Ring Segments

PABLO PÉREZ-MERINO, SERGIO ORTIZ, NICOLAS ALEJANDRE, ALBERTO DE CASTRO, IGNACIO JIMÉNEZ-ALFARO, AND SUSANA MARCOS

• PURPOSE: To analyze corneal and total aberrations using custom-developed anterior segment spectral optical coherence tomography (OCT) and laser ray tracing in keratoconic eyes implanted with intracorneal ring segments (ICRS).

• DESIGN: Evaluation of technology. Prospective study. Case series.

• METHODS: Nineteen keratoconic eyes were measured before and after ICRS surgery. Anterior and posterior corneal topographic and pachymetric maps were obtained pre- and postoperatively from 3-dimensional OCT images of the anterior segment, following automatic image analysis and distortion correction. The pupil center coordinates were used as reference for estimation of corneal aberrations. Corneal aberrations were estimated by computational ray tracing on the anterior and posterior corneal surfaces. Total aberrations were measured using a custom-developed laser ray tracing aberrometer. Corneal and total aberrations were compared in 8 eyes pre- and postoperatively for 4-mm pupils.

• RESULTS: Total and corneal aberrations were highly correlated. Average root mean square of corneal and total high-order aberrations (HOAs) were 0.78 ± 0.35 μm and 0.57 ± 0.39 μm preoperatively, and 0.88 ± 0.36 μm and 0.53 ± 0.24 μm postoperatively (4-mm pupils). The anterior corneal surface aberrations were partially compensated by the posterior corneal surface aberrations (by 8.3% preoperatively and 4.1% postoperatively). Astigmatism was 2.03 ± 1.11 μm preoperatively and 1.60 ± 0.94 μm postoperatively. The dominant HOA aberrations both pre- and postoperatively were vertical coma (Z_3^{-1}), vertical trefoil (Z_3^{-3}), and secondary astigmatism (Z_4^{4}). ICRS decreased corneal astigmatism by 27% and corneal coma by 5%, but on average, the overall amount of HOA did not decrease significantly with ICRS treatment.

• CONCLUSIONS: OCT is a reproducible technique to evaluate corneal aberrations. OCT-based corneal aberrations and ocular aberrations show a high correspondence in keratoconic patients before and after ICRS implantation. ICRS produced a decrease in astigmatism, but on average did not produce a consistent decrease of HOAs. (Am J Ophthalmol 2014;157:116–127. © 2014 by Elsevier Inc. All rights reserved.)

THE QUALITY OF THE IMAGES PROJECTED ON THE retina is determined by the optical properties of the cornea and crystalline lens. In the young eye, the aberrations of the ocular components are generally well tuned, with the aberrations of the lens partly compensating the aberrations of the cornea.[1–8] In diseased eyes such as keratoconus or following certain corneal surgical procedures, this balance is lost as a result of the associated changes in corneal shape.[9–11] Aberrometry techniques, such as Hartmann-Shack or laser ray tracing, have become widely used technologies to measure aberrations in the laboratory and in the clinic. The contribution of the corneal aberrations to the ocular aberrations is typically calculated from the subtraction of corneal aberrations (computed by ray tracing on corneal elevation data) from ocular aberrations. However, the lack of reliable posterior corneal elevation measurements, particularly in highly degraded corneas, has limited a full analysis of the corneal (anterior and posterior surfaces) and total aberrations in keratoconic eyes, before and following treatment.

To date, the analysis of corneal aberrations from both anterior and posterior corneal surfaces has been performed only using Scheimpflug imaging.[12–15] However, several studies have reported a poor repeatability of this technique, especially in irregular corneas.[12,13] This variability could be associated, among other factors, with interpolation errors attributable to meridional sampling approaches, relatively long acquisition times, and errors in optical distortion correction, particularly challenging with highly deformed corneas and in the presence of implants with a refractive index different from that of the cornea.

Spectral-domain optical coherence tomography (OCT) presents several advantages for the measurement of accurate anterior and posterior corneal geometry over other techniques, owing to its high speed and resolution, and the possibility for obtaining 3-dimensional (3-D) corneal

Accepted for publication Aug 21, 2013.

From the Instituto de Óptica "Daza de Valdés", Consejo Superior de Investigaciones Científicas (CSIC) (P.P.M., S.O., N.A., A.D.C., S.M.); and Fundación Jiménez Díaz (N.A., I.J.A.), Madrid, Spain.

Inquiries to Pablo Pérez-Merino, Instituto de Óptica "Daza de Valdés", Consejo Superior de Investigaciones Científicas, C/ Serrano 121, 28006 Madrid, Spain; e-mail: p.perez@io.cfmac.csic.es

0002-9394/$36.00
http://dx.doi.org/10.1016/j.ajo.2013.08.017

maps with a homogeneous rectangular (rather than meridional) sampling.[16–29] OCT provides a direct measurement of corneal elevation, and therefore is free from the skew ray ambiguity present in standard Placido disk topography. Besides, the regular and dense lateral scanning provides higher lateral resolution than typical radial sampling (standard Placido disk) or meridional sampling (Scheimpflug imaging). However, OCT is generally subject to motion artifacts and distortions: fan distortion (arising from the scanning architecture, and resulting in a combination of geometric aberrations, including field distortion, astigmatism, and spherical aberration) and optical distortion (arising from refraction at the optical surfaces). Because of these distortions, OCT images need to be corrected for quantification. Fan (following instrument calibration) and optical distortion (through preceding surfaces) are corrected using 3-D ray tracing analysis.[18–20] Previous work validates the repeatability and accuracy of our spectral OCT system[20] in corneal geometric measurements, and in comparison with Scheimpflug and Placido corneal topography. We have recently demonstrated quantitative anterior segment OCT imaging for surface topography of the cornea and crystalline lens. Besides distortion correction and automatic processing tools, OCT acquisition protocols are optimized to minimize the impact of motion artifacts.[18–23]

In particular, we have presented tools for quantitative anterior and posterior corneal topography in keratoconic corneas before and after treatment with intracorneal ring segments (ICRS), as well as full 3-D characterization of the implanted ICRS.[21,23] While evaluating corneal topography allows monitoring the progression of keratoconus and the potential benefit of the treatment, a better understanding of the impact of the changes of corneal shape (by disease or treatment) is obtained by studying its aberrations, as these determine optical quality. The combined measurements of corneal (anterior and posterior) and total aberrations allow a better understanding of the optical degradation imposed by the corneal deformation in keratoconus and the optical benefit resulting from treatment, as well as the interactions between the aberrations produced by each optical element.

Several studies in the literature have examined total and corneal aberrations in keratoconus.[10,11,30–36] However, although there is evidence that the posterior cornea may be importantly affected in keratoconus,[37] only few studies have considered the posterior corneal shape in the estimation of corneal aberrations.[14,32] Keratoconic[10] and aphakic[5] eyes have in fact been used in the literature as models for cross-validations of total and corneal aberrometry techniques, assuming that total aberrations are primarily driven by the aberrations of the anterior corneal surface. The evaluation of the optical performance in patients implanted with ICRS has been addressed in several studies, which analyzed total and anterior corneal aberrations.[38–42] However, the incorporation of the posterior corneal surface should make those comparisons more accurate. A deeper analysis of the optical changes produced by ICRS (at both the corneal and ocular levels) will help to understand the potential of this technique for the treatment of keratoconus. In this study, we present, for the first time, OCT-based corneal aberrometry and its application in keratoconic patients before and after ICRS implantation. Corneal aberrations were compared with total aberrations measured with laser ray tracing in the same patients. These comparisons allowed evaluating interactive effects of anterior cornea, posterior cornea, and internal aberrations. In addition, the pre- and postoperative optical quality estimated from the measured aberrations was correlated with visual performance. This analysis allowed us to get insights on the potential optical and visual benefits of the ICRS procedure.

SUBJECTS AND METHODS

• **KERATOCONUS PATIENTS:** Nineteen keratoconic eyes of 17 patients (10 male, 7 female) diagnosed by an experienced corneal specialist (N.A.) on the basis of clinical and topographic signs were part of an observational study of ICRS for keratoconus, and were recruited from patients attending the Ophthalmology Service at the Fundación Jiménez-Díaz, Madrid, Spain. The study was revised and approved by the Institutional Review Boards of the Fundación Jiménez-Díaz and followed the tenets of the Declaration of Helsinki. The subjects signed a consent form and they were aware of the nature of the study. Table 1 includes selected descriptive preoperative parameters: keratoconus degree following the Amsler-Krumeich classification, cone location, and maximum anterior corneal curvature (Kmax). The average age of the subjects was 29.3 ± 10.8 years.

• **INTRACORNEAL RING SEGMENT SURGERY:** All surgeries were performed by an experienced surgeon (N.A.). Ferrara-like ICRS were implanted following manual or femtosecond laser–assisted tunnel creation. Table 1 summarizes the specifications of the surgical procedure for ICRS implantation in each patient. Depending on the preoperative corneal topography and refraction, 1 or 2 segments were implanted, equidistantly to the incision site (steepest meridian).

• **CORNEAL ABERRATION ANALYSIS: OPTICAL COHERENCE TOMOGRAPHY:** OCT corneal images of 19 keratoconic eyes were obtained preoperatively and 3 months post ICRS implantation. The spectral OCT instrument, image processing algorithms, and distortion corrections (fan and optical) to obtain anterior and posterior corneal topography from OCT images have been described in detail in previous publications.[17–23]

Briefly, the spectral OCT set-up is based on a fiber-optic Michelson interferometer configuration with a superluminescent diode ($\lambda 0 = 840$ nm, $\Delta\lambda = 50$ nm) as a light

TABLE 1. Descriptive Preoperative Keratoconic Parameters and Surgical Specifications for Intracorneal Ring Segment Implantation

	Preoperative Data			ICRS Parameters					
Eye #	KC Degree	Cone Location	Kmax (D)	ICRS Technique	Optical Zone (mm)	ICRS Thickness (μm)	ICRS Arc Length (deg)	Incision Site (deg)	Planned Depth (μm)
1	III	I-T	52.00	Femtosecond	6	200	210	70	380
2	III	I-C	53.63	Femtosecond	6	a:200; b:200	a:160; b:90	35	360
3	III	I-T	55.20	Femtosecond	6	a:250; b:200	a:120; b:90	100	380
4	III	I-T	56.44	Manual	5	a:250; b:200	a:160; b:120	140	380
5	III	I-T	57.86	Femtosecond	6	a:200; b:200	a:120; b:120	100	380
6	II	I-C	48.58	Femtosecond	6	250	160	110	353
7	III-IV	C	62.35	Manual	5	a:250; b:250	a:160; b:90	120	370
8	III-IV	I-N	58.93	Femtosecond	6	300	210	135	440
9	III-IV	I-C	63.37	Manual	5	a:250; b:250	a:160; b:90	60	380
10	III	I-C	56.15	Manual	5	200	160	50	350
11	III-IV	I-T	59.04	Femtosecond	6	a:250; b:250	a:120; b:120	115	380
12	III-IV	I-C	64.16	Femtosecond	5	300	210	165	380
13	II	I-T	48.64	Femtosecond	6	a:150; b:150	a:120; b:120	75	380
14	II-III	C	56.25	Femtosecond	6	300	150	10	380
15	II	I-N	55.07	Femtosecond	6	250	150	125	375
16	III	C	51.56	Femtosecond	6	300	150	0	380
17	II	I-C	51.63	Femtosecond	6	250	150	140	380
18	II	I-T	52.29	Femtosecond	6	a:300; b:300	a:120; b:120	75	347
19	II	I-T	58.44	Femtosecond	6	250	210	60	380

Cone location notation: C = central; I = inferior; N = nasal; S = superior; T = temporal.
ICRS Thickness and ICRS Arc Length notation: a = left/superior segment; b = right/inferior segment.
Other abbreviations: KC = Keratoconus; Kmax = Maximum anterior corneal curvature; D = diopter; deg = degree.

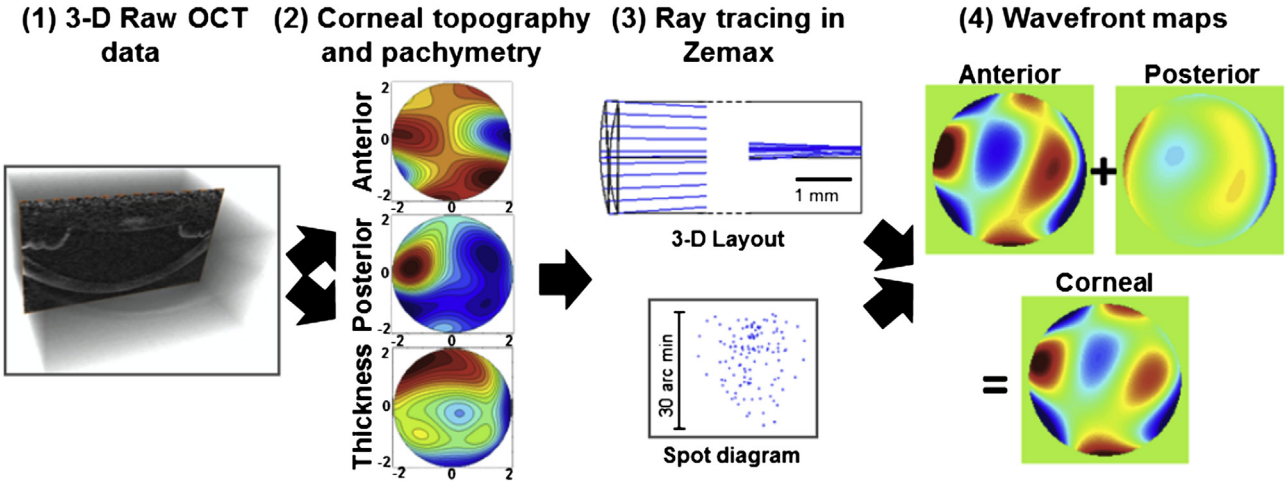

FIGURE 1. Illustration of the computation of corneal aberrations from optical coherence tomography (OCT) distortion-corrected data. The example is shown for a keratoconic eye (Eye 16), preoperatively.

source and a spectrometer consisting of a volume diffraction grating, and a CMOS camera as a detector. The effective acquisition speed is 25 000 A-scans/s. The axial range is 7 mm in depth, resulting in a theoretical pixel resolution of 3.4 μm. The axial resolution is 6.9 μm. Measurements were collected in a 10 × 12-mm area, and consisted of a collection of 50 B-scans composed by 360 A-scans. The total acquisition time of a 3-D data set was 0.72 seconds, which we had previously tested to be sufficiently brief to minimize motion artifacts.

Images were acquired while the subjects fixated a Maltese cross fixation stimulus presented on a mini-display (SVGA OLED LE400; LiteEye Systems, Centennial, Colorado, USA) implemented in a secondary channel. The images

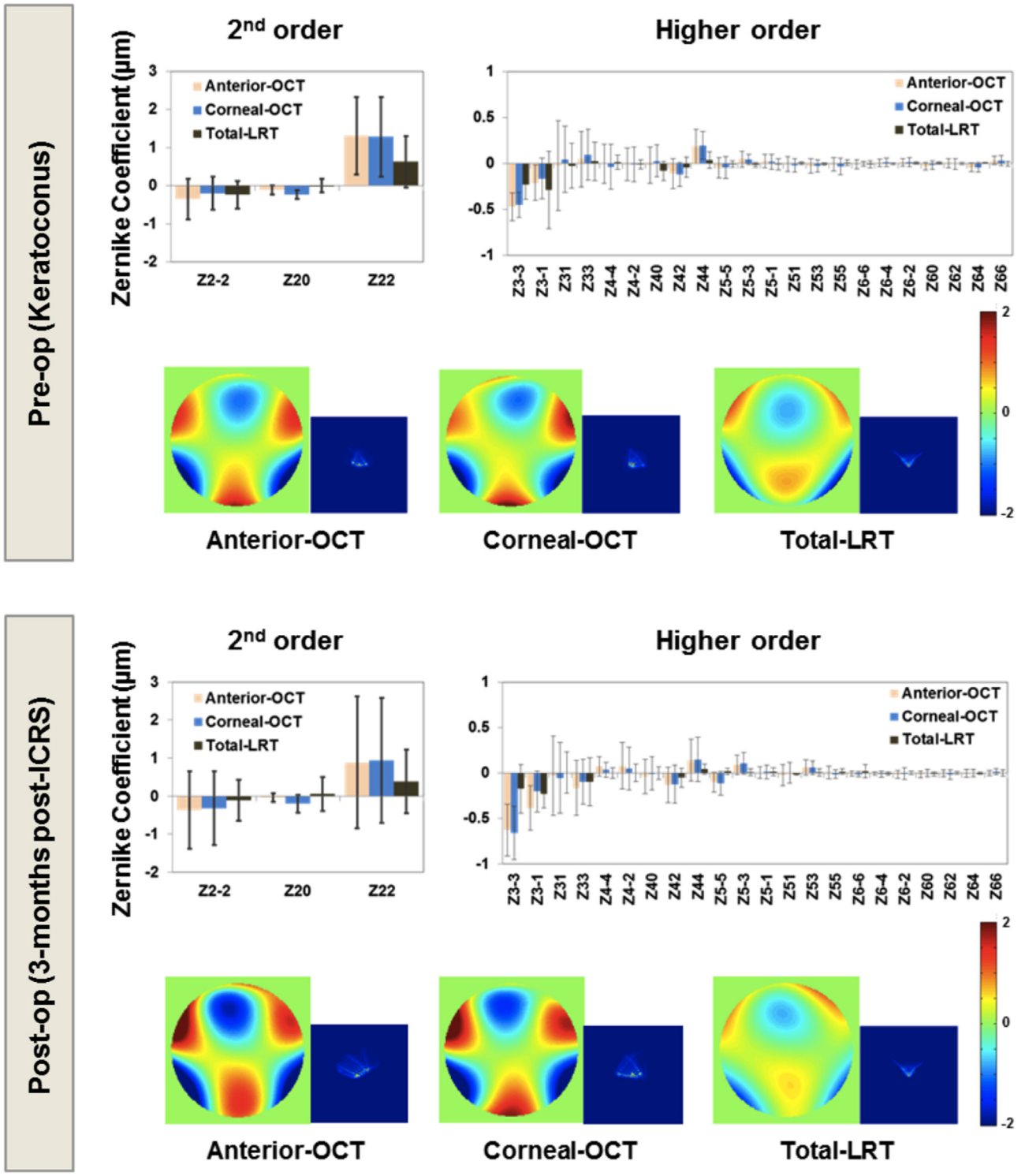

FIGURE 2. Total and corneal Zernike coefficient values (average across 8 eyes), wave aberration maps (calculated from average Zernike coefficients excluding tilt, defocus, and astigmatism) and the simulated point-spread-functions (PSFs) from the wave aberrations (window size: 5 arc min) for keratoconic eyes preoperatively and 3 months post intracorneal ring segment (ICRS) implantation. Data are for 4-mm pupils and referred to the pupil center. (Top) Preoperative data (keratoconus) and (Bottom) postoperative data (3 months post ICRS implantation in keratoconus). OCT = optical coherence tomography; LRT = laser ray tracing.

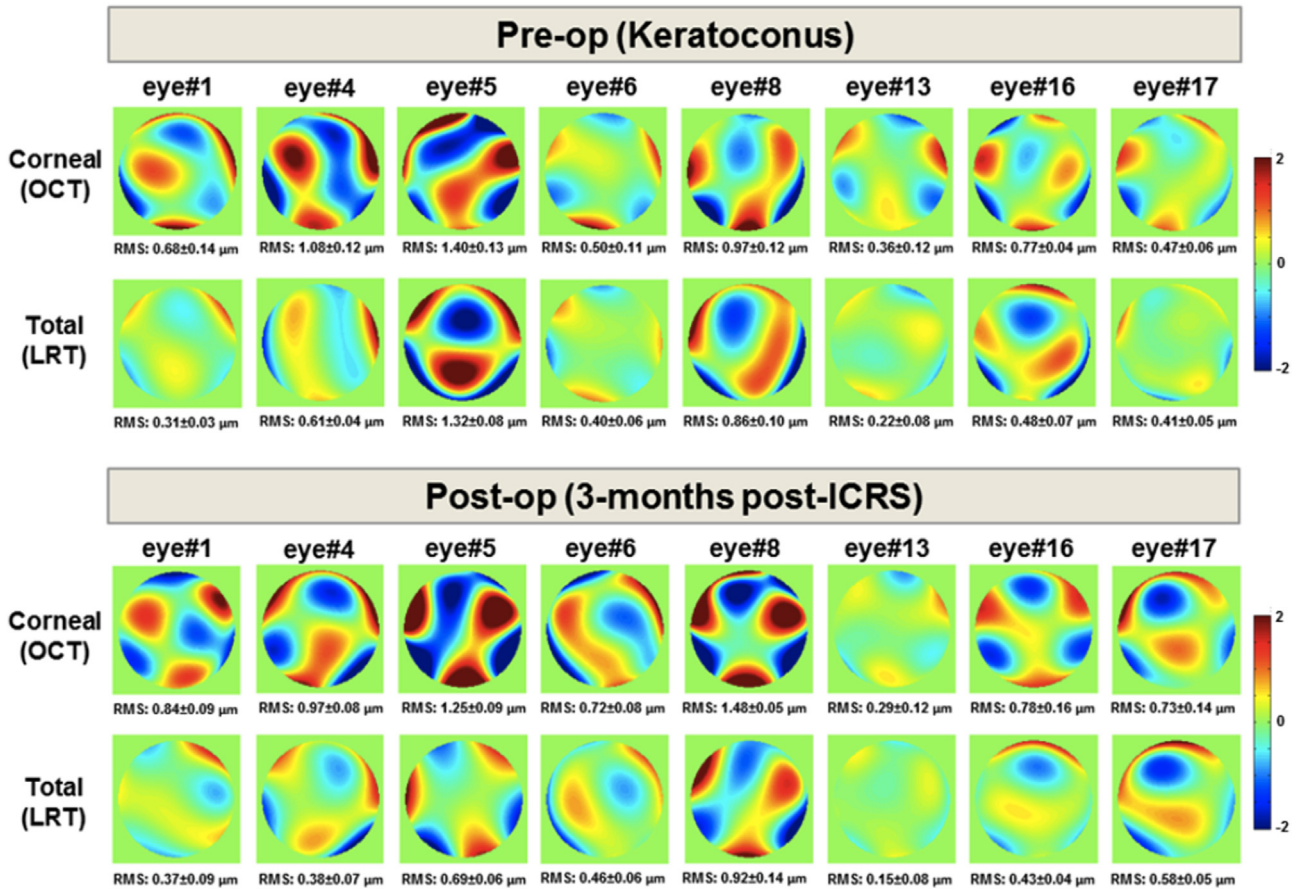

FIGURE 3. Corneal wave aberration maps from optical coherence tomography (OCT) and total wave aberration maps from laser ray tracing in keratoconic eyes and upon intracorneal ring segment (ICRS) treatment. Data are for 4-mm pupil diameter. (Top) Preoperative data (keratoconus). (Bottom) Postoperative data (3 months post ICRS implantation). OCT = optical coherence tomography; LRT = laser ray tracing; RMS = root mean square.

of the cornea were acquired with respect to the anterior corneal specular reflection. Sets of 3-D images were captured approximately 5 seconds after blinking. Five repeated measurements were collected in each condition after inducing mydriasis with 1 drop of tropicamide 1%.

OCT images were de-noised, clustered (cornea, iris, and ICRS), segmented, and corrected from fan and optical distortion correction. The segmented anterior and posterior corneal surfaces were fitted with Zernike polynomial expansion. Corneal thickness maps and the 3-D iris position were also obtained. The iris plane and 3-D coordinates of the pupil center were used for registration of pre- and postoperative data, and as reference for the estimation of corneal aberrations.[21,23]

The pupil center (obtained from the automatically identified iris volume) was used as a reference in the analysis of pre- and postoperative measurements. Corneal elevation maps were reported within the optical zone defined by the ICRS and the natural pupil. The center of the implanted ICRS was obtained from the automatically identified ICRS volume, and its shift from the pupil center was estimated for registration of pre- and postoperative measurements. The rays passing through the ICRS are highly deviated, resulting in halos, and they cannot be accounted for by a standard aberration analysis. For this reason, in this study we have analyzed optical aberrations in a circular 4-mm area concentric with the patient's pupil, in order to ensure quantitative analysis within the optical zone without the influence of ICRS.

Corneal thickness was calculated from direct subtraction of the posterior corneal surface from the anterior corneal surface. Corneal pachymetry is implicitly considered in the estimations of full corneal aberrations, including potential redistributions of corneal thickness (and considering that refractive index remains unchanged). An extensive analysis of corneal pachymetry and longitudinal changes after ICRS can be found in Pérez-Merino and associates.[23]

The elevation data from both corneal surfaces within a central 4-mm pupil diameter area were fitted by Zernike polynomial expansions (up to sixth order) and exported to ZEMAX (Radiant ZEMAX; Focus Software, Tucson, Arizona, USA) for ray tracing analysis. Refractive indices of 1.376 and 1.334 were used for the cornea and aqueous humor, respectively. Wave aberrations were calculated in

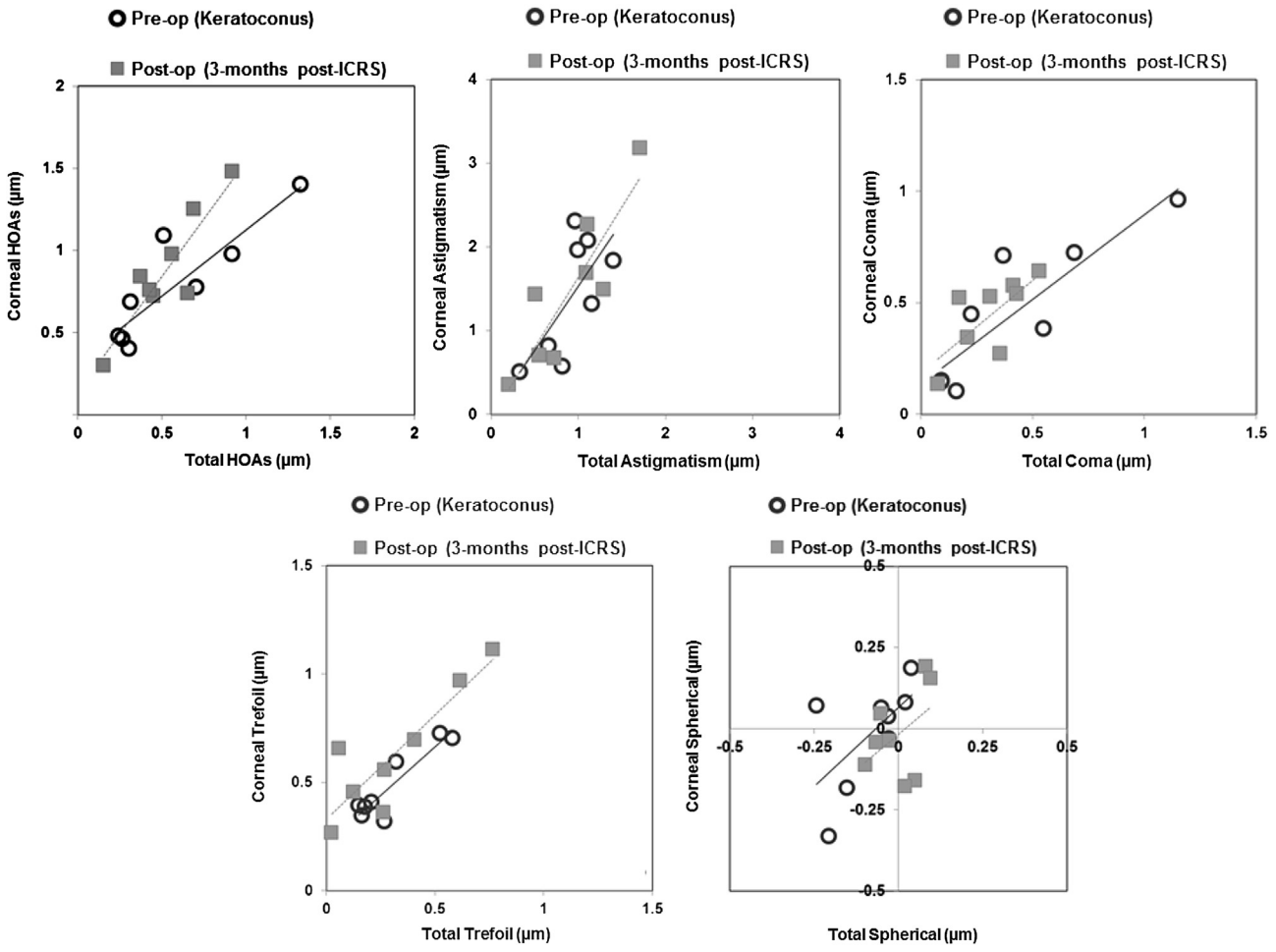

FIGURE 4. Correlation between corneal aberrations (optical coherence tomography) and total aberrations (laser ray tracing) in keratoconic eyes and upon intracorneal ring segment (ICRS) treatment, in terms of root mean square (RMS) for high-order aberrations (Top left), astigmatism (Top middle), coma (Top right), and trefoil (Bottom left), and spherical aberration (Bottom right). Open circles indicate preoperative data (keratoconus) and closed squares postoperative data (3 months post ICRS implantation). Lines are linear regressions to the data.

the pupil plane, placed at 3.47 mm from the anterior corneal surface,[43] by tracing an array of 64 × 64 collimated rays through a 1-surface (anterior cornea only) or 2-surface (anterior and posterior cornea, separated by corneal thickness) eye model. In the 1-surface model, the index after the anterior corneal surface was set to 1.334. The contribution of the posterior corneal surface was obtained from direct subtraction of the anterior corneal surface aberrations from corneal aberrations.[44] Corneal aberrations were analyzed preoperatively and 3 months post ICRS implantation. Figure 1 illustrates the computation of corneal aberrations from OCT data, that is, ray tracing calculation on OCT distortion-corrected corneal surfaces.

• **TOTAL ABERRATION ANALYSIS: LASER RAY TRACING:** Total wave aberrations were measured using custom laser ray tracing, which has been described in detail in a previous study.[45] In brief, an infrared (786-nm) laser beam samples different positions of the pupil sequentially, while a charge-couple device (CCD) camera records the corresponding aerial images of light reflected off the retina. Ray aberrations are obtained by estimating the deviations of the centroids of the retinal spots images corresponding to each entry pupil location with respect to the reference (chief ray). These deviations are proportional to the local derivatives of the wave aberrations. Measurements were done under mydriasis (1 drop 1% tropicamide). The sampling pattern (37 rays in a hexagonal configuration) was adjusted by software to fit a 4-mm pupil centered at the pupil center. The pupil center reference allowed preoperative and postoperative comparisons, and the pupil diameter was selected to guarantee that postoperative measurements fitted the optical zone defined by the inner diameter of the ICRS. Maximum energy exposure was 6.8 µW. Prior to the measurement, the patient adjusted his or her subjective refraction using a Badal optometer.

The Badal system was modified for this study to allow correction of spherical errors up to −12 diopters, frequent in moderate to advanced keratoconus. All measurements were done under foveal fixation of a Maltese cross fixation stimulus. Total wave aberrations were fitted by sixth-order Zernike polynomial expansions following OSA standards. Preoperative and 3-month-post-ICRS total aberrations were measured and analyzed in 8 eyes.

• **OPTICAL QUALITY METRICS:** Wave aberrations were described in terms of individual Zernike coefficients or root mean square (RMS). RMS was used to report the magnitude of high-order aberrations (HOAs) excluding tilt, defocus, and astigmatism, and of certain relevant aberrations (astigmatism, coma, and trefoil). The point-spread function (PSF) and the modulation transfer function (MTF) were computed from Zernike coefficients by means of Fourier optics using routines written in Matlab (MathWorks, Natick, Massachusetts, USA), for 4-mm pupils. Optical quality was described in terms of the visual Strehl metric.[46–48] Visual Strehl was computed as the volume under the visual MTF (obtained from the overlapping of the MTF with the inverse of a general neural transfer function), normalized to diffraction limit. Visual Strehl was evaluated through focus (considering HOAs, and canceling the astigmatic terms). The maximum value of the through-focus visual Strehl curve was obtained as the best-corrected optical quality metric. This optical quality metric has been shown to correlate best with logMAR visual acuity in a normal population.[46,49]

• **VISUAL ACUITY MEASUREMENT:** Visual acuity was measured using a high-contrast Snellen visual acuity test. Patients were tested at a distance of 4 m (13 ft) from the visual acuity chart. All measurements were performed with natural pupils under photopic conditions. Best-corrected visual acuity was obtained for optimal spherical and cylindrical correction with spectacles and given in logMAR units.

• **STATISTICAL ANALYSIS:** Univariate analysis (independent-samples Student *t* test) was used to evaluate differences between preoperative and postoperative measurements. Correlations (Pearson correlation coefficients) were assessed between OCT and laser ray tracing aberration measurements. A *P* value less than .05 was considered statistically significant in all comparisons.

RESULTS

• **LASER RAY TRACING VERSUS OPTICAL COHERENCE TOMOGRAPHY ABERROMETRY:** Corneal and total aberrations were compared in 8 eyes preoperatively and 3 months post ICRS implantation. Figure 2 shows the average coefficients describing the second and HOAs of the whole eye and of the cornea, as well as the corresponding wave aberration maps (excluding tilt, defocus, and astigmatism). The corresponding simulated PSFs for all subjects (average) pre- and postoperatively are also shown. Both pre- and postoperatively, total and corneal aberrations are dominated by astigmatism (eliminated in the maps shown in Figure 2 to allow visualization of higher-order aberrations), vertical coma (Z_3^{-1}), vertical trefoil (Z_3^{-3}), and secondary astigmatism (Z_4^4). Anterior corneal aberrations are slightly higher than those of the whole cornea (including both anterior and posterior surfaces), indicating a compensatory role of the posterior corneal surface. While total and corneal aberrations show quite similar aberration patterns, several total aberration terms tend to be lower than the corresponding corneal aberration terms.

Figure 3 shows individual corneal and total wave aberration maps (excluding tilt, defocus, and astigmatism) for all eyes measured with OCT and with laser ray tracing, preoperatively and 3 months post ICRS implantation. In most eyes, the high-order wave aberration maps are dominated by coma and trefoil. Repeated measurements were highly reproducible within each subject, with average (across all patients and conditions) standard deviations of 0.13 μm (laser ray tracing), 0.17 μm (OCT anterior), and 0.19 μm (OCT corneal) for RMS astigmatism, and of 0.07 μm (laser ray tracing), 0.10 μm (OCT anterior), and 0.11 μm (OCT corneal) for RMS HOA. Total and corneal aberrations show in general a good

TABLE 2. Correlation Parameters Between Corneal (Optical Coherence Tomography) and Total (Laser Ray Tracing) Root Mean Square for High-Order Aberrations, Astigmatism, Coma, and Trefoil, and for Spherical Aberration Preoperatively (Keratoconic Eyes) and Postoperatively (3 Months Post Intracorneal Ring Segment Implantation)

	r[a]	Slope[b]	*P* Value
High-order aberrations			
Pre-op	0.87	0.80	.012[c]
Post-op	0.90	1.40	.001[c]
Astigmatism (Z_2^2 and Z_2^{-2})			
Pre-op	0.71	1.53	.036[c]
Post-op	0.88	1.67	.022[c]
Coma (Z_3^1 and Z_3^{-1})			
Pre-op	0.87	0.75	.132
Post-op	0.64	0.83	.023[c]
Trefoil (Z_3^3 and Z_3^{-3})			
Pre-op	0.91	0.90	.001[c]
Post-op	0.88	0.96	.003[c]
Spherical aberration (Z_4^0)			
Pre-op	0.66	0.97	.197
Post-op	0.44	0.86	.691

Post-op = postoperatively; Pre-op = preoperatively.
[a]r = Pearson product-moment correlation coefficient.
[b]Slope of the regression line.
[c]$P < .05$.

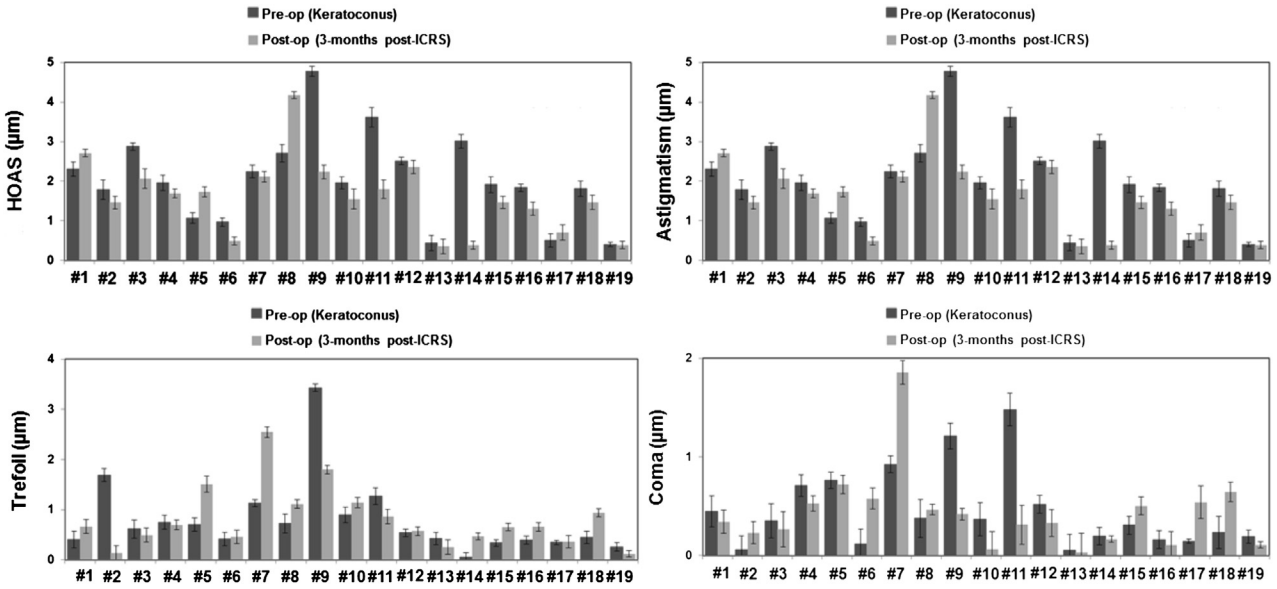

FIGURE 5. Corneal aberrations for all keratoconic eyes and upon intracorneal ring segment (ICRS) treatment. Root mean square for (Top left) high-order aberrations (HOAs), (Top right) astigmatism (Z_2^2 and Z_2^{-2}), (Bottom right) coma (Z_3^1 and Z_3^{-1}), and (Bottom left) trefoil (Z_3^3 and Z_3^{-3}). Data are for 4-mm pupils in keratoconic corneas preoperatively and 3 months post ICRS implantation.

correspondence (except for Eye 5). In most cases total aberrations are lower than corneal aberrations, suggesting a compensatory effect of the crystalline lens. On average, the RMS HOAs were 0.78 ± 0.35 µm (OCT) and 0.57 ± 0.39 µm (laser ray tracing) preoperatively and 0.88 ± 0.36 µm (OCT) and 0.53 ± 0.24 µm (laser ray tracing) postoperatively.

Figure 4 shows the correlation between corneal and total Zernike coefficients (HOA, astigmatism, coma, trefoil, and spherical aberration) for all patients and conditions. Table 2 shows the corresponding correlation coefficients and slopes. Correlations between corneal and total data were statistically significant ($P < .05$) for RMS HOAs (pre- and postoperatively), RMS astigmatism (pre- and postoperatively), RMS trefoil (pre- and postoperatively), and RMS coma (postoperatively). The slopes ranged from 0.75-1.53 (1.07 on average). The highest dispersion (and least significant correlation) was found for spherical aberration, indicative of a patient-dependent compensation of the corneal spherical aberration by the crystalline lens.

• **PRE– AND POST – INTRACORNEAL RING SEGMENT ABERRATIONS:** OCT corneal aberrations were analyzed in 19 eyes preoperatively and 3 months post ICRS implantation. Figure 5 shows corneal (anterior + posterior) aberrations (RMS for HOAs, astigmatism, coma, and trefoil terms) for all subjects. On average, ICRS implantation decreased corneal astigmatism (27%) and produced slight decrease of HOAs (2%) and coma (5%), and slight increase of trefoil (4%). We found slight but not significant correlations between pre- and postoperative astigmatism (r = 0.54, $P = .07$), HOAs (r = 0.55, $P = .89$), coma (r = 0.36, $P = .84$), and trefoil (r = 0.48, $P = .84$). Besides astigmatism, Z_3^{-3}, Z_3^{-1}, Z_3^1, Z_3^3, and Z_4^4 were the predominant corneal aberrations, contributing 19%, 7%, 8%, 8%, and 8% (preoperatively) and 19%, 7%, 9%, 8%, and 5% (postoperatively), respectively, to the overall corneal HOAs.

At the individual level, astigmatism decreased significantly ($P < .006$) 3 months post-ICRS implantation in 14 of 19 eyes (Eyes 2–4, 6, 7, 9–16, 18, and 19). Coma decreased significantly ($P < .03$) in 11 of 19 eyes (Eyes 1, 3–5, 9–14, 16, and 19). Trefoil decreased ($P < .07$) in 7 of 19 eyes (Eyes 2–4, 9, 11, 13, and 19). HOAs decreased significantly ($P < .03$) in 9 of 19 eyes (Eyes 2–4, 9–13, and 19). However, in 4 of 19 eyes (Eyes 1, 5, 8, and 17) astigmatism and HOA increased significantly 3 months post ICRS implantation.

• **VISUAL ACUITY VERSUS OPTICAL QUALITY:** Figure 6 shows best-corrected visual acuity (BCVA) as a function of best visual Strehl, for 4-mm pupil diameter. We found significant correlations between BVCA and visual Strehl both preoperatively (r = −0.51, $P = .02$) and 3 months post ICRS implantation (r = −0.68, $P = .001$). On average, BCVA is slightly but significantly improved with ICRS treatment (preoperative BCVA 0.38 ± 0.19; postoperative BCVA 0.51 ± 0.16; $P = .002$). While there is a displacement of visual Strehl toward higher postoperative values, the change did not reach statistical significance (preoperative visual Strehl: 0.059 ± 0.03; postoperative visual Strehl: 0.063 ± 0.04; $P = .53$).

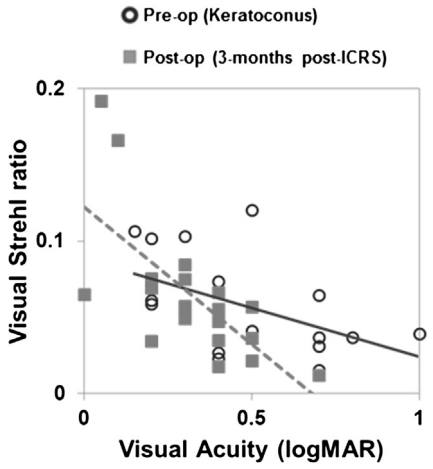

FIGURE 6. Correlation between best-corrected visual acuity (BCVA) and visual Strehl ratio (computed from the visual modulation transfer function for high-order aberrations at best focus, ie, maximum visual Strehl, for 4-mm pupils) in keratoconic eyes and upon intracorneal ring segment (ICRS) treatment. Open circles indicate preoperative data (keratoconus) and closed squares postoperative data (3 months post ICRS implantation). Lines are linear regression to the data (solid line = pre-operatively; dashed line = post-operatively).

• POSTERIOR CORNEAL SURFACE CONTRIBUTION: The posterior corneal surface provides consistent partial compensation of the anterior corneal surface aberration. Figure 7 illustrates the contribution of the posterior corneal surface to the corneal aberrations. On average, the posterior corneal surface compensates 13.9% of astigmatism, 8.3% of HOAs, 16.1% of coma, and 7.7% of trefoil preoperatively; and 4.1% of HOAs, 9.1% of astigmatism, 20.1% of coma, and 3.1% of trefoil 3 months post ICRS implantation. The amount of compensation pre- or postoperatively did not differ significantly.

DISCUSSION

WE HAVE PRESENTED, TO OUR KNOWLEDGE, THE FIRST report of corneal aberrations based on quantitative OCT measurements of corneal elevation maps of anterior and posterior surface. In this study, we measured corneal (OCT-based) and total aberrations (laser ray tracing) in keratoconic eyes preoperatively and 3 months after implantation of ICRS. The high correlation between the measured corneal and total aberrations indicates that OCT alone could be used to describe, to a large extent, the optical quality of keratoconic eyes before and after ICRS treatment, as a result of the predominance of the corneal optics in the overall optical quality of these eyes. OCT-based corneal aberrations (obtained from the anterior and posterior OCT corneal elevation maps) can therefore be obtained along with a number of descriptive evaluation parameters using only OCT, including anterior and posterior corneal topography, corneal pachymetric maps, pupilometry, and 3-D ICRS location (depth and tilt).[20–23] On the other hand, the combined measurements of corneal aberrations and total aberrations in the same patients, as shown for other surgical treatments,[4,5,8–10] provide useful information on the compensatory role of the crystalline lens.

As in previous studies reporting aberrations in keratoconic eyes, we found that astigmatism and coma were the dominant aberrations.[10,11,14,30,32–35] We also found a high contribution of the trefoil vertical Z_3^{-3} (19%) and secondary astigmatism Z_4^4 (8%). In general, total and corneal aberrations showed a good correlation, with the corneal aberrations dominating the ocular wave aberration pattern. These results are in good correspondence with previous reports of corneal and total aberrations in keratoconic patients.[10,30] Despite the high amount of corneal aberrations, total aberrations are consistently lower than corneal aberrations, likely because of compensatory effects of the crystalline lens, particularly for astigmatism and spherical aberration. Several studies in keratoconic eyes have shown that total HOAs are lower than corneal HOAs (by 27.6%[30] to 34.2%[10]), in consistency with the findings of the current study (33.3%).

Several reports point to a compensatory role of the crystalline lens of coma in eyes with normal amounts of aberrations, arising from the off-axis position of the fovea, which generally results in positive corneal and negative internal horizontal coma.[7,8] However, the keratoconic eyes show much higher amount of coma than normal eyes (generally vertical),[10,11,14,30,32–35] induced by the progressive corneal deformation, and such compensatory effect attributable to crystalline lens coma is not expected. However, the difference between anterior corneal and total aberration must arise from the role of the crystalline lens as well as from the posterior corneal surface. Dubbelman and associates[50,51] reported an average compensation of 31% of the anterior corneal astigmatism and 3.5% of the anterior corneal coma by the posterior corneal surface in a normal population. In keratoconus, Chen and Yoon[32] reported an average compensation of approximately 20% of anterior corneal astigmatism and coma by the posterior corneal surface. In this study, we found a larger compensation of coma (16.1% preoperative and 20.1% postoperative), but smaller compensation of astigmatism (13.9% preoperative and 9.1% postoperative). In addition, some compensation occurred for trefoil terms (7.7% preoperative and 3.1% postoperative). Overall, the posterior cornea compensated, on average, 8.3% (preoperative) and 4.1% (postoperative) of the aberrations of the anterior cornea, with no significant differences in the amount of compensation pre- and postoperatively. Differences with respect to the anterior/posterior corneal balances reported in the literature on normal subjects may arise from the large topographic differences (in anterior and posterior corneal

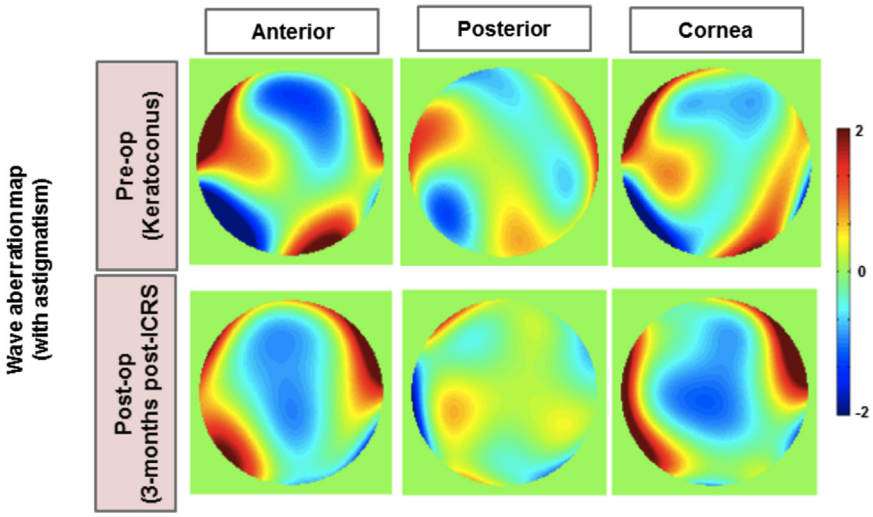

FIGURE 7. Examples of anterior, posterior, and corneal wave aberration maps in a keratoconic eye and upon intracorneal ring segment (ICRS) treatment (Eye 19). Upper panels show preoperative data (keratoconus) and lower panels postoperative data (3 months post ICRS implantation).

surfaces) of keratoconic (both pre- and postoperatively) with respect to normal eyes.

Intracorneal ring segments are becoming an increasingly used alternative for treatment of keratoconus progression.[52–54] While the literature reporting clinical visual performance outcomes is relatively extensive, few studies evaluate aberrations following ICRS treatment.[38–42] Piñero and associates[40] reported a significant improvement in anterior corneal astigmatism (3.21 ± 2.16 μm preoperative, 2.50 ± 1.73 μm post ICRS) and a reduction of coma-like anterior corneal aberrations (3.46 ± 1.86 μm preoperative, 2.94 ± 1.45 μm post ICRS) and of anterior corneal HOAs (3.73 ± 1.97 μm preoperative, 3.24 ± 1.44 μm post ICRS) 3-months post ICRS implantation, for 6-mm pupils. In contrast, Chalita and Krueger[38] reported an increase in ocular HOA in the ICRS-implanted eye, when compared to the nontreated fellow eye. On average, 3 months post ICRS implantation we found very small changes (average values not statistically significant) in HOAs (mean decrease of 2%), coma (mean decrease of 5%), and trefoil (mean increase of 4%) after ICRS surgery. Furthermore, we found a larger decrease (although it did not reach statistical significance, on average) of astigmatism (27%). At the individual level, we have found a reduction of asymmetric aberration terms and an overall significant decrease of aberrations in several patients (up to a decrease of 2.63 μm in astigmatism, 1.17 μm in coma, or 1.63 μm for trefoil). Inter-subject variability in the optical response to ICRS may arise from differences in the corneal biomechanical properties across patients, and from the difficulty of the treatment to control simultaneously the topographic and refractive outcomes. In general, the aims of reducing astigmatism, reducing coma, or flattening the cornea (to improve contact lens fitting) were met, at least partially, in most patients, although a full simultaneous reduction of both overall astigmatism and HOA was not generally achieved.

The optical findings were in good agreement with visual performance measurements in this group of patients. As found in previous studies in normal subjects,[46,49] we also found significant correlations between optical quality for HOAs (described by the visual Strehl optical quality metric at best focus) and visual quality (BCVA), supporting the value of aberration measurements in predicting visual performance. The small overall improvement in visual acuity is consistent with the small improvement in optical quality.

To sum up, this study presents, to our knowledge, the first report of 3-D OCT-based corneal aberrometry. The technique has been applied to evaluate optical aberrations in keratoconic eyes preoperatively and 3 months post ICRS implantation. Both OCT-based whole corneal aberrations and laser ray tracing ocular aberrations have been measured and found to be highly correlated. The combined estimation of anterior corneal aberrations, whole corneal aberrations, and measured total aberrations allowed evaluation of the compensatory role of the posterior cornea and of the crystalline lens. ICRS implantation produced a decrease in astigmatism, but on average did not produce a consistent decrease of higher-order aberrations, which is consistent with the small increase of visual acuity following treatment. The effect of the ICRS implantation on optical quality varied across patients. The quantitative optical and geometric data, all obtained from the same OCT instrument, can be used to study keratoconus and to improve the current nomograms for ICRS implantation[55] and postoperative assessment of the outcomes.

ALL AUTHORS HAVE COMPLETED AND SUBMITTED THE ICMJE FORM FOR DISCLOSURE OF POTENTIAL CONFLICTS OF INTEREST. The authors indicate the following financial disclosure(s): Spanish patent: Procedure to calibrate and correct the scan distortion of an optical coherence tomography system, P201130685 (Sergio Ortiz, Susana Marcos, Damian Siedlecki, and Carlos Dorronosoro). The research leading to these results has received funding from the European Research Council under the European Union's Seventh Framework Programme (FP7/2007-2013)/ERC Grant Agreement no. 294099. This study has also been supported by the Spanish Government (grants FIS2011-25637, CEN-2091021) to S. Marcos. Contributions of authors: conception and design of the study (P.P.M., S.O., N.A., S.M.); analysis and interpretation (P.P.M., S.O., N.A., A.C., S.M.); writing the article (P.P.M., S.M.); critical revision of the article (S.O., N.A., A.C., I.J.A.); final approval of the article (P.P.M., S.O., N.A., A.C., I.J.A., S.M.); data collection (P.P.M., N.A.); provision of materials, patients, or resources (N.A., I.J.A., S.M.); statistical expertise (P.P.M., S.O.); obtaining funding (S.M.); literature search (P.P.M., S.O.). The authors also acknowledge Unidad Asociada IO-CSIC/FJD. The authors thank Lucie Sawides for scientific discussions and technical advice.

REFERENCES

1. Sivak JG, Kreuzer RO. Spherical aberration of the crystalline lens. *Vision Res* 1983;23(1):59–70.
2. Guirao A, Redondo M, Artal P. Optical aberrations of the human cornea as a function of age. *J Opt Soc Am A Opt Image Sci Vis* 2000;17(10):1697–1702.
3. Artal P, Guirao A. Contribution of the cornea and the lens to the aberrations of the human eyes. *Opt Lett* 1998;23(21):1713–1715.
4. Artal P, Guirao A, Berrio E, Williams DR. Compensation of corneal aberrations by the internal optics in the human eye. *J Vis* 2001;1(1):1–8.
5. Barbero S, Marcos S, Merayo-Lloves J. Corneal and total aberrations in a unilateral aphakic patient. *J Cataract Refract Surg* 2002;28(9):1594–1600.
6. He JC, Gwiazda J, Thorn F, Held R. Wave-front aberrations in the anterior corneal surface and the whole eye. *J Opt Soc Am A Opt Image Sci Vis* 2003;20(7):1155–1163.
7. Kelly JE, Mihashi T, Howland HC. Compensation of corneal horizontal/vertical astigmatism, lateral coma, and spherical aberration by internal optics of the eye. *J Vis* 2004;4(4):262–271.
8. Marcos S, Rosales P, Llorente L, Barbero S, Jiménez-Alfaro I. Balance of corneal horizontal coma by internal optics in eyes with intraocular artificial lenses: evidence of a passive mechanism. *Vision Res* 2008;48(1):70–79.
9. Marcos S, Barbero S, Llorente L, Merayo-Lloves J. Optical response to LASIK surgery for myopia from total and corneal aberration measurements. *Invest Ophthalmol Vis Sci* 2001;42(13):3349–3356.
10. Barbero S, Marcos S, Merayo-Lloves J, Moreno-Barriuso E. Validation of the estimation of corneal aberrations from videokeratography in keratoconus. *J Refract Surg* 2002;18(3):263–270.
11. Maeda N, Fujikado T, Kuroda T, et al. Wavefront aberrations measured with Hartmann-Shack sensor in patients with keratoconus. *Ophthalmology* 2002;109(11):1996–2003.
12. Shankar H, Taranath D, Santhirathelagan CT, Pesudovs K. Repeatability of corneal first-surface wavefront aberrations measured with Pentacam corneal topography. *J Cataract Refract Surg* 2008;34(5):727–734.
13. Read SA, Collins MJ, Iskander DR, Davis BA. Corneal topography with Scheimpflug imaging and videokeratography: comparative study of normal eyes. *J Cataract Refract Surg* 2009;35(6):1072–1081.
14. Piñero DP, Alió JL, Alesón A, Escaf M, Miranda M. Pentacam posterior and anterior corneal aberrations in normal and keratoconic eyes. *Clin Exp Optom* 2009;92(3):297–303.
15. Nakagawa T, Maeda N, Kosaki R, et al. Higher-order aberrations due to the posterior corneal surface in patients with keratoconus. *Invest Ophthalmol Vis Sci* 2009;50(6):2660–2665.
16. Huang D, Swanson EA, Lin CP, et al. Optical coherence tomography. *Science* 1991;254(5035):1178–1181.
17. Grulkowski I, Gora M, Szkulmowski M, et al. Anterior segment imaging with spectral OCT system using a high-speed CMOS camera. *Opt Express* 2009;17(6):4842–4858.
18. Ortiz S, Siedlecki D, Grulkowski I, et al. Optical distortion correction in optical coherence tomography for quantitative ocular anterior segment by three-dimensional imaging. *Opt Express* 2010;18(3):2782–2796.
19. Ortiz S, Siedlecki D, Remon L, Marcos S. Three-dimensional ray tracing on Delaunay-based reconstructed surfaces. *Appl Opt* 2009;48(20):3886–3893.
20. Ortiz S, Siedlecki D, Pérez-Merino P, et al. Corneal topography from spectral optical coherence tomography (sOCT). *Biomed Opt Express* 2011;2(12):3232–3247.
21. Ortiz S, Pérez-Merino P, Alejandre N, Gambra E, Jimenez-Alfaro I, Marcos S. Quantitative OCT-based corneal topography in keratoconus with intracorneal ring segments. *Biomed Opt Express* 2012;3(5):814–825.
22. Ortiz S, Pérez-Merino P, Gambra E, de Castro A, Marcos S. In vivo human crystalline lens topography. *Biomed Opt Express* 2012;3(10):2471–2488.
23. Pérez-Merino P, Ortiz S, Alejandre N, Jiménez-Alfaro I, Marcos S. Quantitative OCT-based longitudinal evaluation of intracorneal ring segment implantation. *Invest Ophthalmol Vis Sci* 2013;54(9):6040–6051.
24. Lai MM, Tang M, Andrade EM, et al. Optical coherence tomography to assess intrastromal corneal ring segments depth in keratoconic eyes. *J Cataract Refract Surg* 2006;32(11):1860–1865.
25. Li Y, Meisler DM, Tang M, et al. Keratoconus diagnosis with optical coherence tomography pachymetry mapping. *Ophthalmology* 2008;115(12):2159–2166.
26. Li Y, Tang M, Zhang X, Salaroli CH, Ramos JL, Huang D. Pachymetric mapping with Fourier-domain optical coherence tomography. *J Cataract Refract Surg* 2010;36(5):826–831.
27. Zhao M, Kuo AN, Izzat JA. 3D refraction correction and extraction of clinical parameters from spectral domain optical coherence tomography of the cornea. *Opt Express* 2010;18(9):8923–8936.
28. Tang M, Chen A, Li Y, Huang D. Corneal power measurement with Fourier-domain optical coherence tomography. *J Cataract Refract Surg* 2010;36(12):2115–2122.

29. Karnowski K, Kaluzny BJ, Szkulmowski M, Gora M, Wojtkowski M. Corneal topography with high-speed swept source OCT in clinical examination. *Biomed Opt Express* 2011;2(9):2709–2720.
30. Schlegel Z, Lteif Y, Bains HS, Gatinel D. Total, corneal, and internal ocular optical aberrations in patients with keratoconus. *J Refract Surg* 2009;(10 Suppl):S951–S957.
31. Sabesan R, Yoon G. Visual performance after correcting higher order aberrations in keratoconic eyes. *J Vis* 2009;9(5):1–10.
32. Chen M, Yoon G. Posterior corneal aberrations and their compensation effects on anterior corneal aberrations in keratoconic eyes. *Invest Ophthalmol Vis Sci* 2008;49(12):5645–5652.
33. Saad A, Gatinel D. Evaluation of total and corneal wavefront high order aberrations for the detection of forme fruste keratoconus. *Invest Ophthalmol Vis Sci* 2012;53(6):2978–2992.
34. Jinabhai A, Radhakrishnan H, O'Donnell C. Repeatability of ocular aberration measurements in patients with keratoconus. *Ophthalmic Physiol Opt* 2011;31(6):588–594.
35. Mihált K, Kovács I, Kránitz K, Erdei G, Németh J, Nagy ZZ. Mechanism of aberration balance and the effect on retinal image quality in keratoconus: optical and visual characteristics of keratoconus. *J Cataract Refract Surg* 2011;37(5):914–922.
36. Piñero DP, Alio JL, Barraquer RI, Michael R, Jiménez R. Corneal biomechanics, refraction, and corneal aberrometry in keratoconus: an integrated study. *Invest Ophthalmol Vis Sci* 2010;51(4):1948–1955.
37. Tomidokoro A, Oshika T, Amano S, Higaki S, Maeda N, Miyata K. Changes in anterior and posterior corneal curvatures in keratoconus. *Ophthalmology* 2000;107(7):1328–1332.
38. Chalita MR, Krueger RR. Wavefront aberrations with the Ferrara intrastromal corneal ring in a keratoconis eye. *J Refract Surg* 2004;20(6):823–830.
39. Piñero DP, Alio JL, El Kady B, et al. Refractive and aberrometric outcomes of intracorneal ring segments for keratoconus: mechanical versus femtosecond-assisted procedures. *Ophthalmology* 2009;116(9):1675–1687.
40. Piñero DP, Alio JL, Teus MA, Barraquer RI, Uceda-Montañés A. Modelling the intracorneal ring segement effect in keratoconus using refractive, keratometric and aberrometric data. *Invest Ophthalmol Vis Sci* 2010;51(11):5583–5591.
41. Piñero DP, Alió JL, El Kadi B, Pascual I. Corneal aberrometric and refractive performance of 2 intrastromal corneal ring segments models in early and moderate ectatic disease. *J Cataract Refract Surg* 2010;36(1):102–109.
42. Hamdi IM. Optical and topographic changes in keratoconus after implantation of Ferrara intracorneal ring segments. *J Refract Surg* 2010;26(11):871–880.
43. Szalai E, Berta A, Hassan Z, Módis L Jr. Reliability and repeatability of swept-source Fourier-domain optical coherence tomography and Scheimpflug imaging in keratoconus. *J Cataract Refract Surg* 2012;38(3):485–494.
44. Sicam VA, Dubbelman M, van der Heijde RG. Spherical aberration of the anterior and posterior surfaces of the human cornea. *J Opt Soc Am A Opt Image Sci Vis* 2006;23(3):544–549.
45. Llorente L, Diaz-Santana L, Lara-Salcedo D, Marcos S. Aberrations of the human eye in visible and near infrared illumination. *Optom Vis Sci* 2003;80(1):26–35.
46. Cheng X, Bradley A, Thibos LN. Predicting subjective judgement of best focus with objective image quality metrics. *J Vis* 2004;4(4):310–321.
47. Thibos LN, Hong X, Bradley A, Applegate RA. Accuracy and precision of objective refraction from wavefront aberrations. *J Vis* 2004;4(4):329–351.
48. Iskander DR. Computational aspects of the visual Strehl ratio. *Optom Vis Sci* 2006;83(1):57–59.
49. Schoneveld P, Pesudovs K, Coster DJ. Predicting visual performance from optical quality metrics in keratoconus. *Clin Exp Optom* 2009;92(3):289–296.
50. Dubbelman M, Sicam VA, van der Heijde GL. The shape of the anterior and posterior surface of the aging human cornea. *Vision Res* 2006;46(6-7):993–1001.
51. Dubbelman M, Sicam VA, van der Heijde GL. The contribution of the posterior surface to the coma aberration of the human cornea. *J Vis* 2007;7(7):1–8.
52. Colin J, Cochener B, Savary G, Malet F. Correcting keratoconus with intracorneal rings. *J Cataract Refract Surg* 2000;26(8):1117–1122.
53. Siganos D, Ferrara P, Chatznikolas K, Bessis N, Papastergiou G. Ferrara intrastromal corneal rings for the correction of keratoconus. *J Cataract Refract Surg* 2002;28(11):1947–1951.
54. Alió JL, Shabayek MH, Artola A. Intracorneal ring segments for keratoconus correction: long-term follow-up. *J Cataract Refract Surg* 2006;32(6):978–985.
55. Kling S, Marcos S. Finite-element modeling of intrastromal ring segment implantation into a hyperelastic cornea. *Invest Ophthalmol Vis Sci* 2013;54(1):881–889.

Biosketch

Pablo Pérez-Merino, MSc in Vision Sciences graduated at the University of Valladolid, Valladolid, Spain. He is a research associate and PhD student at the Visual Optics and Biophotonic Lab in the Optic Institute (Consejo Superior de Investigaciones Científicas, CSIC). His research interests are focused on aberrometry, optical coherence tomography (OCT) and clinical applications for the anterior segment of the eye.